Available online at www.sciencedirect.com
ScienceDirect
European Journal of Pharmaceutics and Biopharmaceutics 69 (2008) 1160–1170
European Journal of Pharmaceutics and Biopharmaceutics
www.elsevier.com/locate/ejpb

Research paper

# Application of PGSTE-NMR technique to characterize the porous structure of pharmaceutical tablets

Virginie Busignies [a], Patrice Porion [b], Bernard Leclerc [a], Pierre Evesque [c], Pierre Tchoreloff [a,*]

[a] Centre d'études Pharmaceutiques, Université Paris Sud-XI, 92296 Châtenay-Malabry Cedex, France
[b] Centre de Recherche sur la Matière Divisée, CNRS – Université d'Orléans, 45071 Orléans Cedex 2, France
[c] Laboratoire de Mécanique: Sols – Structure – Matériaux, CNRS – Ecole Centrale de Paris, 92296 Châtenay-Malabry Cedex, France

Received 31 October 2007; accepted in revised form 11 February 2008
Available online 19 February 2008

**Abstract**

Direct compaction of pharmaceutical tablets is a complex process that results in a heterogeneous density distribution inside the compact. In the present study, we have used a non-invasive and non-destructive technique: the pulsed-gradient stimulated-echo (PGSTE) NMR method to access to topological information (connectivity, tortuosity) about the porous structure of tablets obtained with three different pharmaceutical excipients: the microcrystalline cellulose, the lactose and the anhydrous calcium phosphate. These materials were chosen since their mechanical properties under pressure are highly differentiated. To probe the pore space with the PGSTE-NMR technique, the tablets were initially impregnated with silicone oil that is NMR sensitive ($^1$H NMR). The time-dependent apparent self-diffusion coefficient was measured over a suitable range of diffusion time in the directions perpendicular and parallel to the compression axis, from which the tortuosity factor and the anisotropy of the porous structure can be studied. These results show that the porous structure varies with pressure and depends on the excipient behaviour under pressure. Then, this work demonstrates that PGSTE-NMR could be an alternative and very interesting technique to obtain useful information on the structural properties of such compacted materials.


*Keywords:* Compaction; Tablets; Porosity; Compressibility; Pulsed-gradient stimulated-echo NMR; Diffusion; Self-diffusion coefficient; Tortuosity; Anisotropy

## 1. Introduction

Direct compaction is commonly used to produce pharmaceutical tablets. The step of compaction corresponds to the densification of powder. Compaction can lead to a heterogeneous density distribution and produce a porous structure which depends on the precise behaviour of powder during compaction, on the interparticle frictions and on die wall frictions [1]. The consequence is that the density variations in the pharmaceutical tablets may be important and may affect the tablet's properties. The first study on density variation in the tablets was performed by Train [1] in 1956. More recently, experimental works using innovative techniques such as X-ray microtomography have been published to continue those of Train [2–5]. If heterogeneity of density is observed in tablets, this also leads to a heterogeneity of the porous structure. More, the distributions of density and porosity are important to consider because they affect the local properties of tablets the and finally influence the mechanical properties, the behaviour during post-compression operations and disintegration.

Some techniques allow to study the porosity of tablets, like nitrogen adsorption or mercury porosimetry [6]. These techniques provide information about the porous volume

* Corresponding author. EA 401, Matériaux et Produits de Santé, IFR-141, Centre d'études Pharmaceutiques, Université Paris Sud-XI, 5 rue Jean-Baptiste Clément, 92296 Châtenay-Malabry Cedex, France. Tel.: +33 1 46 83 56 11; fax: +33 1 46 83 59 63.
*E-mail address:* pierre.tchoreloff@u-psud.fr (P. Tchoreloff).

0939-6411/$ - see front matter © 2008 Elsevier B.V. All rights reserved.
doi:10.1016/j.ejpb.2008.02.008

**Nomenclature**

| | |
|---|---|
| $\mathbf{D}$ | Self-diffusion tensor in the orthogonal frame ($Oxyz$) |
| $D_0$ | Bulk self-diffusion coefficient of silicone oil ($m^2\ s^{-1}$) |
| $D_x(\Delta)$ | Self-diffusion coefficient in the direction perpendicular to the compression axis ($m^2\ s^{-1}$) |
| $D_z(\Delta)$ | Self-diffusion coefficient in the direction parallel to the compression axis ($m^2\ s^{-1}$) |
| $D_x^\infty$ | Macroscopic value of $D_x(\Delta)$ ($m^2\ s^{-1}$) |
| $D_z^\infty$ | Macroscopic value of $D_z(\Delta)$ ($m^2\ s^{-1}$) |
| $\mathbf{e}_i$ | Unitary vector along the direction ($Oi$) |
| $\mathbf{e}_i^T$ | Transposed vector of $\mathbf{e}_i$ |
| $g$ | Intensity of the pulsed magnetic field gradient ($T\ m^{-1}$) |
| ($Ox$) | Direction perpendicular to the compression axis |
| ($Oz$) | Direction parallel to the compression axis |
| $P_y$ | Mean yield pressure (MPa) |
| $T_1$ | Longitudinal relaxation time (s) |
| $T_2$ | Transverse relaxation time (s) |
| $\gamma$ | Gyromagnetic ratio of the proton nucleus, $2.6752 \times 10^8\ rad\ s^{-1}\ T^{-1}$ |
| $\Delta$ | Diffusion time (s) |
| $\delta$ | Duration of the pulsed magnetic field gradient (s) |
| $\varepsilon$ | Porosity of tablets |
| $\theta$ | Tortuosity |
| $\lambda$ | Diffusion anisotropy factor |
| $\sigma$ | Compaction pressure (MPa) |
| $\tau_x$ and $\tau_z$ | Tortuosity factor of the pore space in the direction perpendicular and parallel to the compression axis |

of the sample without any directional attention. For example, from the nitrogen adsorption experiments, it is possible to obtain the specific surface area (BET model) [7] or the pore size distribution (BJH model) [8] of a porous material, but this technique does not allow access to a topological characterization of the porous space like the tortuosity of the network pores. To study the porous structure of the pharmaceutical tablets, we have used the pulsed-gradient stimulated-echo (PGSTE) NMR experimental technique [9]. In other scientific domains, NMR methods are used to characterize various porous media or complex fluids [10–13]. Nevertheless, it is not already the case of pharmaceutical tablets' porosity. The PGSTE-NMR technique is non-destructive and does not involve the introduction of a chemical tracer. For the tablets, it consists in studying the self-diffusion process of a molecular fluid when this one is confined to their porous networks. These measurements and their behaviours allow to determine the pore structure when the results are compared to those ones observed when the molecules are not confined to the porous network of the material. This last situation corresponds to the diffusion process in a bulk fluid which is characterized by the bulk self-diffusion coefficient of the fluid (noted $D_0$). When the fluid is confined to a porous medium, diffusion is restricted by the solid surfaces bounding the pore space, and this induces a decrease of the self-diffusion coefficient as compared to the bulk solvent. Then, PGSTE-NMR technique allows to observe the restricted diffusion process by the measurement of the self-diffusion coefficient along any given direction of anisotropic porous space using a microimaging probehead with gradient coils in three perpendicular directions. By this PGSTE-NMR method, like with the nitrogen adsorption experiments, only materials with an entirely open porous structure can be explored and characterized correctly.

The purpose of this work is to characterize the porous structure of tablets obtained by uniaxial compaction, the most used process in pharmaceutical technology. First, three pharmaceutical excipients (microcrystalline cellulose, lactose and anhydrous calcium phosphate) were compacted and their compressibility properties determined. Second, the study of the self-diffusion process of a molecular fluid inside the pore space was performed for tablets compacted under various pressures, in the directions perpendicular and parallel to the compaction axis. These results were linked with the tabletting mechanical behaviour of the three excipients. Finally, the tortuosity factor and the anisotropy of the porous structure were deduced from the PGSTE-NMR experimental results and analyzed.

## 2. Materials and methods

### 2.1. Excipients

The materials were a microcrystalline cellulose (Vivapur 12®, 5601210932, JRS, Germany), a partly amorphous lactose (Fast Flo®, 8500042062, Foremost, USA) and an anhydrous calcium phosphate (A TAB®, GW930187, Rhodia, France). These excipients were chosen as models of materials with different behaviour in terms of fragmentation and deformability propensity [14–16]. The 100–180 μm sieve fractions were used in all the cases. The main physical characteristics of the three excipients were previously determined [17] and are reported in Table 1. The three excipients were mixed with 0.5% (microcrystalline cellulose and lactose) or 1% (calcium phosphate) by weight of magnesium stearate (NF-BP-MF2, Akcros Chemicals v.o.f., Netherlands) with a Turbula mixer (Type T2C, Willy A Bachofen, Switzerland) at 50 rpm for 5 min. Before use, the fractions and the mixtures with magnesium stearate were stored in a closed chamber at $48 \pm 6\%$ of relative humidity for at least three days.

Table 1
Physical properties and characteristics of the three excipients (values are expressed as mean ± standard deviation)

| Excipient | Apparent particular density (g/cm$^3$)[a] | Mean particle size (V%) (μm)[b] | Specific surface area (m$^2$/g)[c] |
|---|---|---|---|
| Calcium phosphate (A TAB®) | 2.7682 ± 0.0004 | 162 ± 35 | 9.847 ± 0.212 |
| Lactose (Fast Flo®) | 1.5287 ± 0.0003 | 134 ± 36 | 0.221 ± 0.003 |
| Microcrystalline cellulose (Vivapur 12®) | 1.5380 ± 0.0007 | 152 ± 48 | 1.127 ± 0.009 |

[a] Helium pycnometry (AccuPyc 1330, Micromeritics); $n = 3$, materials with magnesium stearate.
[b] Laser diffraction granulometry (Coulter LS 230, $\lambda = 750$ nm), $n = 3$.
[c] Nitrogen adsorption, B.E.T. method (Coulter SA 3100); $n = 3$, materials with magnesium stearate.

### 2.2. Study of the compressibility of the three excipients

Cylindrical tablets of excipients mixed with magnesium stearate were obtained using an eccentric instrumented Frogerais OA tabletting press. The powders were manually poured into the cylindrical die (section of 1 cm$^2$ and height of 1 cm) and compacted under 280 MPa. The press and the method of compaction were described in more details in a previous paper [18]. Heckel's plots [19,20] were generated from the compaction pressures ($\sigma$) and the porosity data ($\varepsilon$) collected during the compaction. The relationship defined by Heckel is similar to

$$\ln(1/\varepsilon) = k \cdot \sigma + A \quad (1)$$

where $k$ and $A$ are constants.

In the case of pharmaceutical products, the plots are usually divided into two parts: the first step corresponding to rearrangement and/or fragmentation, this step is followed by a linear step. From the linear part of the curve, the mean yield pressure ($P_y$ in MPa) is obtained for the three excipients. It is defined by $1/k$ and is related to the behaviour of the material.

### 2.3. Compaction of the excipients for the PGSTE-NMR study

The tablets used for the NMR experiments must be introduced in an NMR tube which has an inner diameter of 8.5 mm. Then, specific tablets were produced with the mixtures of the excipients and magnesium stearate. An eccentric instrumented Frogerais OA tabletting press was used, but in this case it was equipped with a punch of 8 mm in diameter. The height of the cylindrical die was kept constant and equal to 1 cm. The target compaction pressures used were 40 (only for microcrystalline cellulose), 80, 150 and 200 MPa. After compaction, the compacts were stored for at least three days in a closed chamber at a relative humidity of 48 ± 6% to relax. Mean porosity of relaxed tablets was calculated from the apparent particular density, the dimensions and the weight of each tablet. The evolution of the porosity with compaction pressure is shown in Fig. 1.

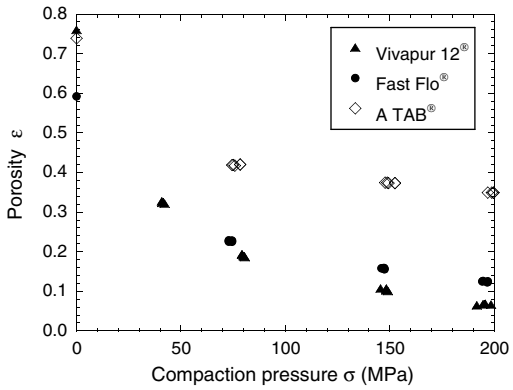


Fig. 1. Evolution of tablet porosity ($\varepsilon$) *versus* compaction pressure ($\sigma$, MPa) for the three excipients. Key: ▲, microcrystalline cellulose; ●, lactose; ◇, anhydrous calcium phosphate.

### 2.4. PGSTE-NMR technique

#### 2.4.1. Oil impregnation of the tablets

In this study, the structure of the porosity was indirectly characterized by the observation of the modification of the diffusion process of a molecular fluid which entirely saturates the pore space of the tablets. Then, it is necessary to find a filling fluid with several properties: it must be NMR sensitive ($^1$H NMR) and it must not interact with the sample, *i.e.* it does not modify the porous structure by chemical reaction, dissolution or swelling. In this work, a fluid organic silicone oil was used (polydimethylsiloxane, Rhodorsil 47V20, Prolabo, France). Before the NMR experiments, the tablet was totally saturated by the silicone oil which was introduced in the porous space by a simple impregnation process induced by the capillary effect. This silicone oil is characterized by a bulk self-diffusion coefficient ($D_0$) of $2.73 \times 10^{-11}$ m$^2$ s$^{-1}$ at 296 K. Some PGSTE-NMR measurements were performed after different durations of impregnations to control the modification of the porous structure.

#### 2.4.2. PGSTE-NMR measurements

The self-diffusion coefficients of the silicone oil molecules have been measured by using the pulsed-gradient stimulated-echo (PGSTE) NMR method [21,22]. In porous materials, the confined fluids are often characterized by a large difference of values between the two relaxation times $T_1$ and $T_2$ and one has $T_1 \gg T_2$ where $T_1$ and $T_2$ are the longitudinal and transverse relaxation times, respectively, [9]. In that case, the standard pulsed-gradient spin-echo (PGSE) NMR sequence [21] is not suitable to measure with good accuracy the self-diffusion coefficient at long diffusion time $\Delta$ due to the short $T_2$ value. In this study, the typical

relaxation measurements of the silicone oil molecules confined to the pharmaceutical tablets of different excipients give a ratio $T_1/T_2 \approx 50$ (with $T_1 \approx 1000$ ms and $T_2 \approx 20$ ms). For this reason, we have used a modified PGSE-NMR sequence, the PGSTE-NMR sequence, [22] which allows to significantly enhance the echo signal in such experimental conditions. In such NMR measurements, the proton $^1$H spins of the silicone oil molecules are labeled at time $t = 0$ with respect to their positions in a given direction ($Oi$) by applying a pulse of magnetic field gradient along this direction; after an evolution time $\Delta$ called diffusion time, a second pulse of magnetic field gradient is then applied. This second pulse cancels the effect of the first one, unless the spins have moved during the time $\Delta$ along the same direction ($Oi$). If the spins have diffused along this chosen direction ($Oi$), the second gradient pulse does not refocus all the spins signal and the echo intensity is less intense. This decrease of the echo amplitude is a function of the self-diffusion coefficient $D$, and the echo attenuation $E(q,\Delta)$ measured using this method is given by the following equation:

$$E(q,\Delta) = \frac{I(q,\Delta)}{I(0,\Delta)} = \exp[-4\pi^2 q^2 \mathbf{e}_i^T \mathbf{D} \mathbf{e}_i (\Delta - \delta/3)] \quad (2)$$

where $q = \gamma g \delta / 2\pi$, with $g$ is being intensity of the pulsed magnetic field gradient, $\delta$ its duration, $\mathbf{e}_i$ the unitary vector along the chosen direction ($Oi$), $\mathbf{e}_i^T$ its transposed vector, $\Delta$ the diffusion time and $\gamma$ the gyromagnetic ratio of the proton, $\mathbf{D}$, the self-diffusion tensor, $I(q,\Delta)$ and $I(0,\Delta)$ being the echo intensities, respectively, measured with and without the magnetic field gradient $g$. The PGSTE-NMR sequence is represented in Fig. 2a. It consists in applying to the sample, along an arbitrary direction $\mathbf{e}_i$, a magnetic field $B(x_i)$ which depends linearly on the position $x_i$. This fixes the Larmor frequency which then depends on the position of the molecules along the direction $\mathbf{e}_i$. This magnetic field $B(x_i)$ is the superposition of a constant magnetic field $B_0$ (the static magnetic field) and of a second magnetic field defined through its gradient $g$. This last one is applied during two short lapses of time of the same duration $\delta$ starting at $0 < t < \tau_1$ and $t + \tau_1 + \tau_2$ so that $t + \delta < \tau_1$. Three $\pi/2$ radio-frequency pulses are used and applied, respectively, at times 0, $\tau_1$ and $\tau_1 + \tau_2$. An adequate phase cycling is used to select the right coherence transfer pathway (see Fig. 2b) and produce only one spin-echo at time $2\tau_1 + \tau_2$, called stimulated spin-echo. With this sequence, the diffusion time corresponds to the delay $\Delta = \tau_1 + \tau_2$ and consequently during the most of the diffusion time $\Delta$ corresponding to the delay $\tau_2$, the magnetization of the spins is then aligned along the static magnetic field $B_0$ and subjected only to the longitudinal relaxation $T_1$. With this sequence, the higher value of $\Delta$ is experimentally limited by the $T_1$ value. In this work, for all excipients, the upper value of the diffusion time was taken at 5000 ms, it corresponds to five times the longitudinal relaxation time ($T_1 \approx 1000$ ms). Since the same pulse sequence with the same coherence pathway is used to record the echo intensities with ($I(q,\Delta)$) and without ($I(0,\Delta)$) magnetic field gradient, for a given diffusion time $\Delta$, they are both affected by the same relaxation mechanisms of the silicone oil molecules, leading to the same echo attenuation $I(0,\Delta)$. This one is thus proportional to $\exp(-2\tau_1/T_2)\exp(-\tau_2/T_1)$. As a consequence, the echo attenuation $E(q,\Delta)$ which is measured at a given diffusion time $\Delta$ as a function of the magnetic field gradient strengths $g$ depends only on the diffusion process of the molecular fluid inside the porous space as mentioned in Eq. (2).

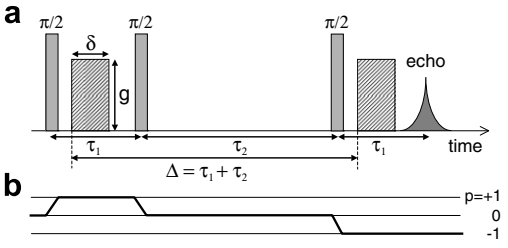


Fig. 2. (a) PGSTE-NMR sequence used for the measurement of the self-diffusion coefficient. The three $\pi/2$ pulses produce a stimulated spin-echo at time $2\tau_1 + \tau_2$. Between the second and third pulse, during the $\tau_2$ period, the magnetization is stored along the static magnetic field $B_0$ parallel to ($Oz$) axis and therefore subjected only to the longitudinal relaxation time $T_1$. The diffusion time is $\Delta = \tau_1 + \tau_2$, a gradient of magnetic field $g$ is applied in the direction $\mathbf{e}_i$ during a lapse $\delta$ between $t = 0$ and $t = \tau_1$ and repeated after a delay $\Delta$; (b) Coherence transfer pathway ($p = 0 \rightarrow +1 \rightarrow 0 \rightarrow -1$) resulting from an adequate phase cycling to take into account only the stimulated echo.

All measurements were performed on a Bruker DSX100 spectrometer operating at 100 MHz for the proton (2.35 T superconducting magnet), and a microimaging probehead (Micro5 Bruker) with gradient coils in three perpendicular directions was used to generate magnetic field gradient in any arbitrary direction $\mathbf{e}_i$. The temperature was fixed at 296 K. For a given direction $\mathbf{e}_i$, the self-diffusion coefficient is extracted from a series of measurements involving different $g$ values varying between 0 and 1.5 T m$^{-1}$ (16 steps), with the $\delta$ duration fixed at 5 ms. The self-diffusion coefficient $D$ is obtained by a simple linear fit of $\ln(E(q,\Delta))$ as a function of $4\pi^2 q^2 \Delta$ (see Fig. 3 for examples). For each diffusion time $\Delta$, the self-diffusion coefficients were measured only along two distinct perpendicular directions: the directions perpendicular and parallel to the compression axis ($Oz$) (see Fig. 4) due to the cylindrical symmetry of the tablets. These two coefficients were noted as $D_x(\Delta)$ and $D_z(\Delta)$, respectively.

## 3. Results and discussion

### 3.1. Heckel's plot

The mean yield pressures ($P_y$) were determined from the linear part of Heckel's plots (Fig. 5). The limits of the linear zone are, respectively, 50 and 150 MPa for microcrystalline cellulose, 50 and 210 MPa for lactose, 100 and 280 MPa for anhydrous calcium phosphate. The mean yield pressures

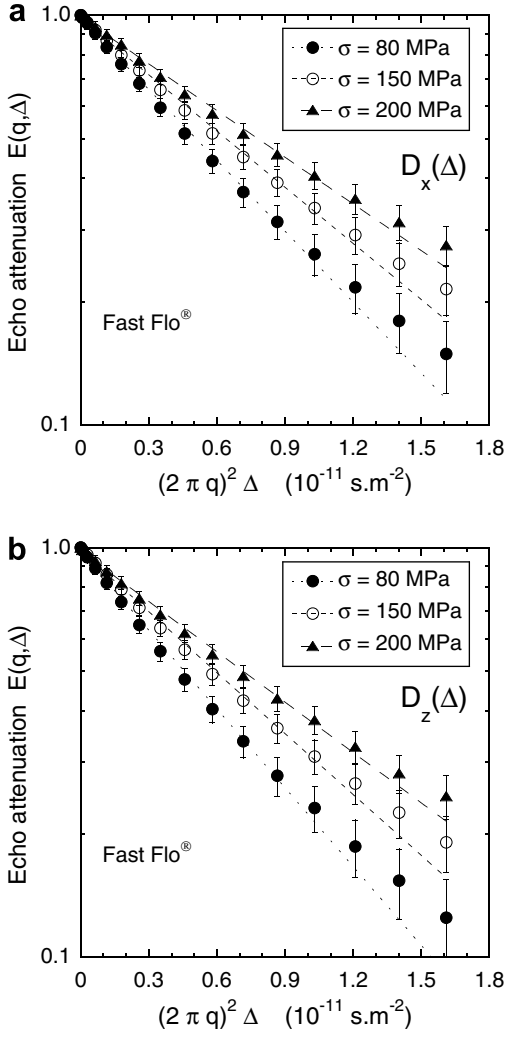


Fig. 3. Examples of echo amplitude attenuation $E(q,\Delta)$ as a function of $4\pi^2q^2\Delta$ ($q=\gamma g\delta/2\pi$) measured for the lactose for a diffusion time $\Delta=1$s at different compaction pressure ($\sigma$, MPa). The self-diffusion coefficients $D$ are calculated by least-squares fitting (straight lines). (a) $D_x(\Delta)$ along the direction perpendicular to the compression axis, $\mathbf{e}_i=(1,0,0)$; (b) $D_z(\Delta)$ along the direction parallel to the compression axis, $\mathbf{e}_i=(0,0,1)$.

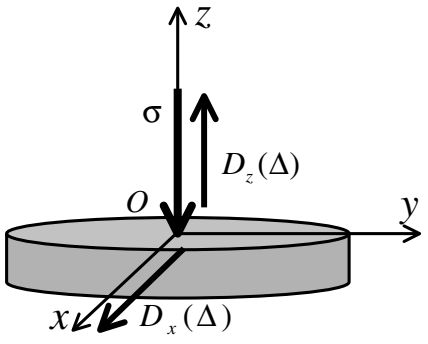


Fig. 4. Reference axis used for the measurements of the diffusion process in the tablets and definition of the $D_x(\Delta)$ and $D_z(\Delta)$ self-diffusion coefficients.

illustrate the differences in densification behaviour. Microcrystalline cellulose is a plastic material with $P_y=59$ MPa.

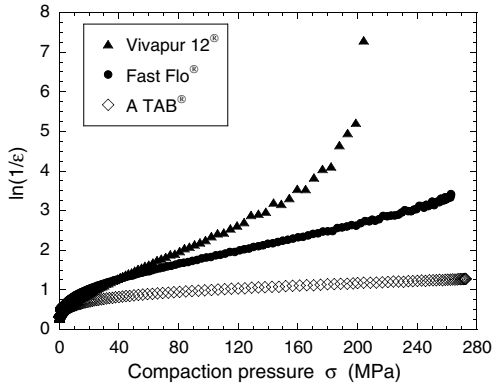


Fig. 5. Heckel's plots of the three excipients mixed with magnesium stearate. Key: ▲, microcrystalline cellulose; ●, lactose; ◇, anhydrous calcium phosphate.

Anhydrous calcium phosphate deforms by fragmentation ($P_y=672$ MPa). Lactose has an intermediate densification behaviour shown by a mean yield pressure of 118 MPa. These results are in good accordance with the previous works [14–16].

### 3.2. Diffusion in the porous space

As already mentioned, due to the cylindrical symmetry of the tablets, the self-diffusion coefficients were measured along the directions perpendicular and parallel to the compression axis as function of the diffusion time $\Delta$ (varying between 30 and 5000 ms) according to the following procedure. Direct measurements of $I(0,\Delta)$ and $I(q,\Delta)$ have been obtained for different values of $q$ and $\Delta$. From these data, one can calculate the echo attenuation $E(q,\Delta)=I(q,\Delta)/I(0,\Delta)$ for each $q$ and $\Delta$. For instance, Fig. 3 reports typical examples of the variations $E(q,\Delta)$ *versus* $4\pi^2q^2\Delta$ at $\Delta=1$ s, obtained with lactose compressed at 80, 150 and 200 MPa in the two orthogonal directions ($Ox$) and ($Oz$). This attenuation $E(q,\Delta)$ should obey Eq. (2), as explained already, from which one can get the self-diffusion coefficient $D_x(\Delta)$ or $D_z(\Delta)$. All the results are shown in Figs. 6 and 7.

Firstly, for all excipients, at a given diffusion time, the two self-diffusion coefficients $D_x(\Delta)$ and $D_z(\Delta)$ decrease when the compaction pressure is increased. From the evolution of the porosity described in Fig. 1, this means that the diffusion process is slowed down when the porosity decreases. Secondly, for all compaction pressures, the self-diffusion coefficient decreases continuously from 30 ms to about 2000 ms to reach an asymptotic value. This dependence of $D$ on the diffusion time is the fingerprint of the restricted diffusion phenomena which is often observed in porous materials [23]. Indeed, at very short time $\Delta$, the molecules do not have enough time to explore the structure and to encounter the walls of the pores, $D$ is then equal to $D_0$, the one for non-confined silicone oil. Consequently, one expects that the bulk diffusion coefficient $D_0$ shall be obtained at $\Delta\to 0$, in the limit when the molecules of liquid do not undergo physi- or chemi-sorption at the solid sur-

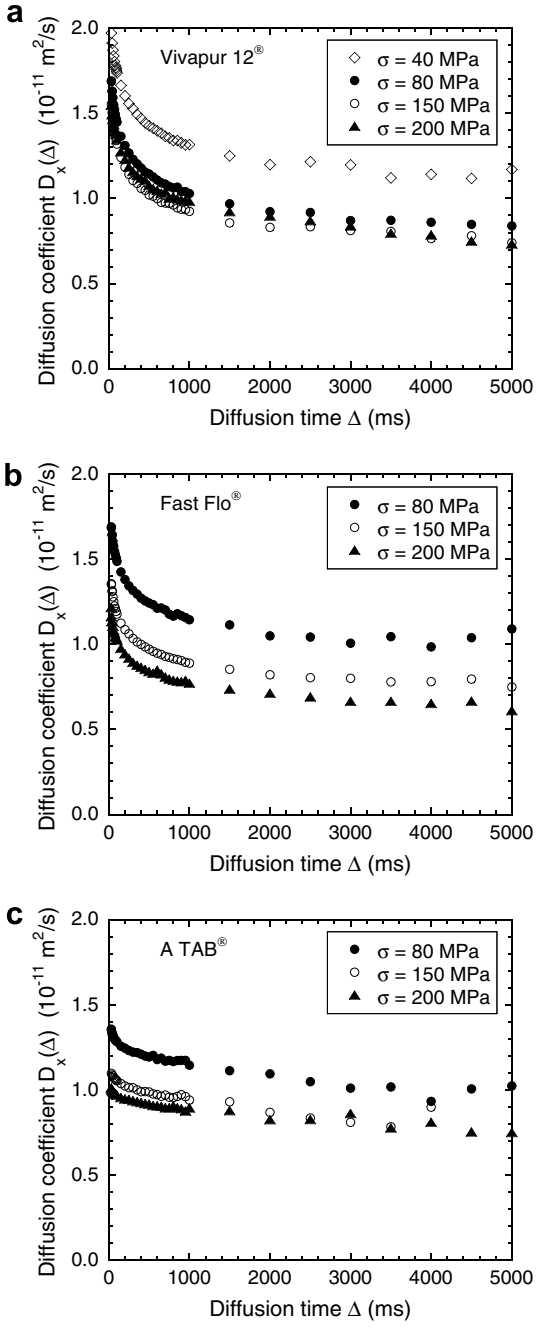


Fig. 6. Evolution of proton self-diffusion coefficient $D_x(\Delta)$ with the diffusion time ($\Delta$) in the direction ($Ox$) perpendicular to the compression axis for tablets obtained under different compaction pressure ($\sigma$, MPa); (a) microcrystalline cellulose, (b) lactose and (c) anhydrous calcium phosphate.

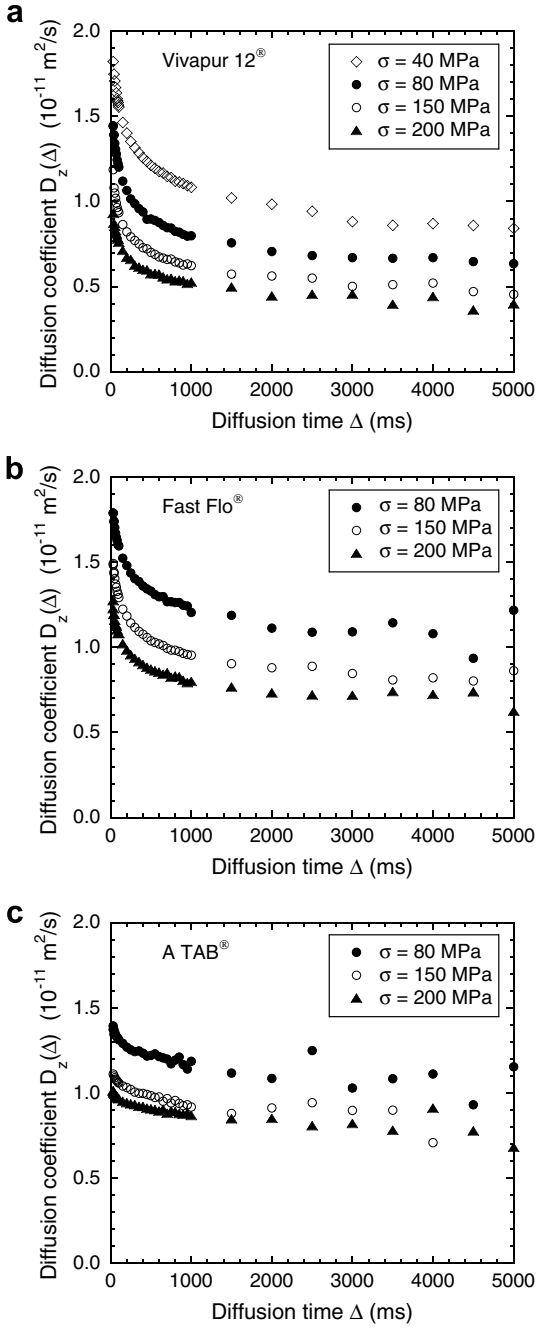


Fig. 7. Evolution of proton self-diffusion coefficient $D_z(\Delta)$ with the diffusion time ($\Delta$) in the direction ($Oz$) parallel to the compression axis for tablets obtained under different compaction pressure ($\sigma$, MPa); (a) microcrystalline cellulose, (b) lactose and (c) anhydrous calcium phosphate.

face of the pore and in the limit of a large volume-to-surface ratio. Due to the limitations of PGSTE-NMR technique, which impose a diffusion time $\Delta$ greater than few milliseconds, it is impossible to explore this regime at very small times. In this study, the smaller diffusion time was taken equal to 30 ms, in order to obtain a significant attenuation of $E(q,\Delta)$ for an accurate evaluation of the self-diffusion coefficient. For large enough time, the molecules begin to encounter the walls and their pathway is restricted: in this regime, restriction of motion is then imposed whose statistics depends on the diffusion length $\xi$ travelled, hence on the diffusion time $\Delta$ at which the NMR measure is performed. This phenomenon reduces the value of the self-diffusion coefficient: $D$ is smaller than $D_0$. The bigger $\Delta$, the smaller $D$, until the time $\Delta$ is sufficiently large so that the molecules have explored the whole representative volume of sample for the diffusion process. Finally, at long time $\Delta$, the effect of the pore space structure is averaged and

$D$ does not depend on $\Delta$ anymore. In these samples, this regime occurs for $\Delta$ greater than 2–3 s. These asymptotic values of the self-diffusion coefficients are noted $D_i^\infty$ with $i \in \{x,z\}$ and they are evaluated as the mean value of $D_i(\Delta)$ for a time diffusion varying between 3 and 5 s in the case of the microcrystalline cellulose or 2 and 4 s in the case of anhydrous calcium phosphate and lactose. Assuming that the cross-over between the two last regimes appears for a critical value of the diffusion time $\Delta_c$ equal to 3 s, it is possible to calculate a characteristic diffusion length $\ell_i = \sqrt{2D_i^\infty \Delta_c}$ and the size of the representative elementary volume (REV) for the different samples $V_{\mathrm{REV}} = \pi(\ell_x/2)^2\ell_z$ as seen by its diffusion transport properties. In this expression, we make the hypothesis that due to the cylindrical symmetry of the sample, the REV volume is a cylinder (radius $\ell_x/2$ and height $\ell_z$). The results are summarized in Table 2. At a scale larger than this REV size, the tablets can be seen as homogeneous materials for the diffusion process and the self-diffusion coefficients $D_i^\infty$ correspond to the macroscopic values of those. These results in terms of characteristic diffusion length $\ell_i$ can also be observed in Figs. 8 and 9, where the evolutions of the self-diffusion coefficients are represented as a function of the diffusion length $\xi = \sqrt{2D(\Delta)\Delta}$. These characteristic diffusion lengths $\ell_i$ correspond to the values of $\xi$ for which the asymptotic regime is reached.

For the microcrystalline cellulose and the lactose, $D_i^\infty$ decrease continuously as expected when the compaction pressure increases. This behaviour is the fingerprint that the porosity and the connectivity become more and more reduced when the powder bed is tabletted with a higher pressure. On the contrary, for the anhydrous calcium phosphate tablets, $D_i^\infty$ values become almost constant from 150 MPa. This signs that the porosity reaches a constant value for the highest compaction pressure. This is in accordance with the evolution of the porosity in Fig. 1 and with the previous work in which the minimal porosity observed is 31% with anhydrous phosphate tablets and 6% with lactose and microcrystalline cellulose tablets [24]. Concerning the difference of $D_i^\infty$ values according to the direction of the measurement, for microcrystalline cellulose, $D_x^\infty$ is widely higher than $D_z^\infty$ for all compaction pressures. For lactose and anhydrous calcium phosphate, $D_z^\infty$ is slightly higher or equal to $D_x^\infty$ depending on the pressure.

For each excipient, it is interesting to compare the evolution of $D_x(\Delta)$ and $D_z(\Delta)$. Indeed, due to the different compaction behaviour, the results depend on the excipient studied. For microcrystalline cellulose, the highest variations of $D_x(\Delta)$ and $D_z(\Delta)$ are observed between 40 and 80 MPa. In reference to the previous section, the mean yield pressure is within this range of pressures. Consequently, the change of particles deformation behaviour seems to correspond to a modification of the porous structure. In addition, for all compaction pressures, $D_x(\Delta)$ is higher than $D_z(\Delta)$. This means that the diffusion process in the tablets is easier along the radial direction ($Ox$) than along the longitudinal one ($Oz$). This anisotropy of the pore space results from a specific deformation of the particles induced by the plastic behaviour of the microcrystalline cellulose material under an uniaxial compression. For the lactose and the anhydrous calcium phosphate that are, respectively, intermediate and brittle excipients, the higher variations of $D_x(\Delta)$ and $D_z(\Delta)$ appear between 80 and 150 MPa. In the case of the lactose, it is in the range of its mean yield pressure. This variation could be explained by a change of the nature of particle deformation. Contrary to the microcrystalline cellulose, $D_x(\Delta)$ is almost equal to $D_z(\Delta)$. This means that the pore space must be isotropic.

### 3.3. Characterization of the pore space by its tortuosity factor

The concept of tortuosity was originally proposed by Carman in 1937 [25]. The tortuosity $\theta$, as defined by Carman, characterizes the trajectory length of the fluid in a porous material. With this definition, the real length $L^*$ covered

Table 2
Asymptotic values $D_x^\infty$ and $D_z^\infty$ of the self-diffusion coefficient corresponding to the behaviour for the long diffusion times $\Delta$ and evaluations of the representative elementary volume size $V_{\mathrm{REV}}$ as function of the compaction pressure for the three excipients

| Excipient compaction pressure (MPa) | $D_x^\infty$ ($10^{-12}$ m$^2$/s) | $\ell_x$ (μm) | $D_z^\infty$ ($10^{-12}$ m$^2$/s) | $\ell_z$ (μm) | $V_{\mathrm{REV}} = \pi(\ell_x/2)^2\ell_z$ (μm$^3$) |
|---|---|---|---|---|---|
| *Calcium phosphate* | | | | | |
| 80 | 10.22 | 7.83 | 11.13 | 8.17 | 393.40 |
| 150 | 8.402 | 7.10 | 8.732 | 7.24 | 286.65 |
| 200 | 8.208 | 7.02 | 8.350 | 7.08 | 274.03 |
| *Lactose* | | | | | |
| 80 | 10.25 | 7.84 | 11.03 | 8.14 | 392.96 |
| 150 | 7.969 | 6.91 | 8.489 | 7.14 | 267.76 |
| 200 | 6.770 | 6.37 | 7.268 | 6.60 | 210.34 |
| *Microcrystalline cellulose* | | | | | |
| 40 | 11.50 | 8.30 | 8.628 | 7.19 | 389.02 |
| 80 | 8.576 | 7.17 | 6.576 | 6.28 | 253.56 |
| 150 | 7.807 | 6.84 | 4.923 | 5.43 | 199.53 |
| 200 | 7.804 | 6.84 | 4.111 | 4.97 | 182.62 |

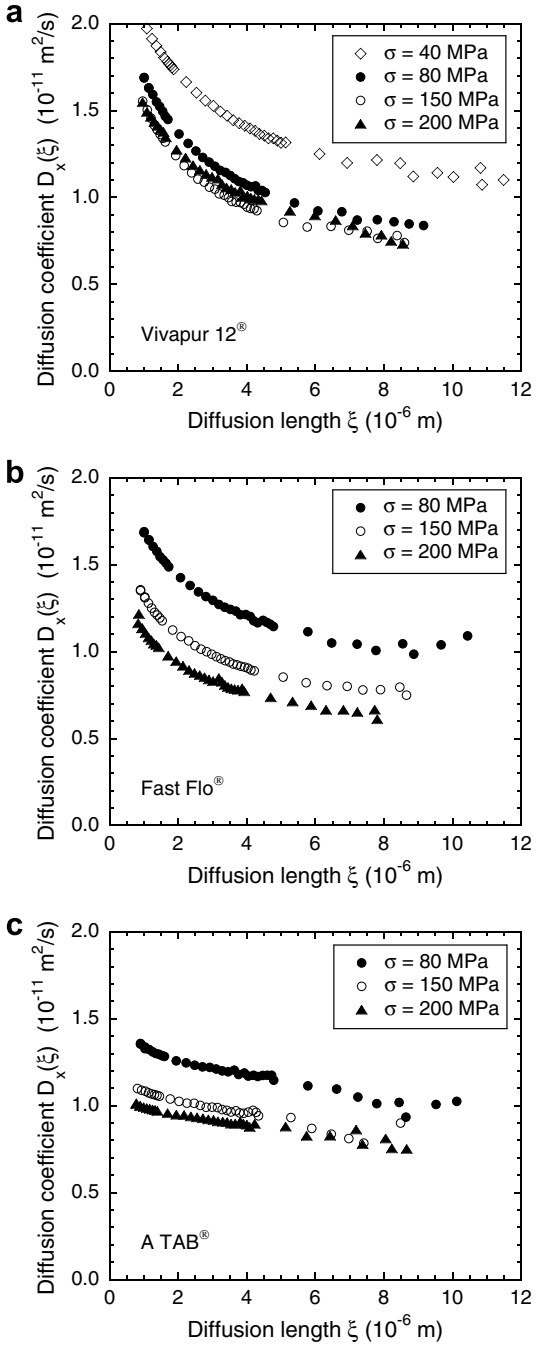


Fig. 8. Evolution of proton self-diffusion coefficient $D_x(\xi)$ with the diffusion length ($\xi$) in the direction ($Ox$) perpendicular to the compression axis for tablets obtained under different compaction pressure ($\sigma$, MPa); (a) microcrystalline cellulose, (b) lactose and (c) anhydrous calcium phosphate.

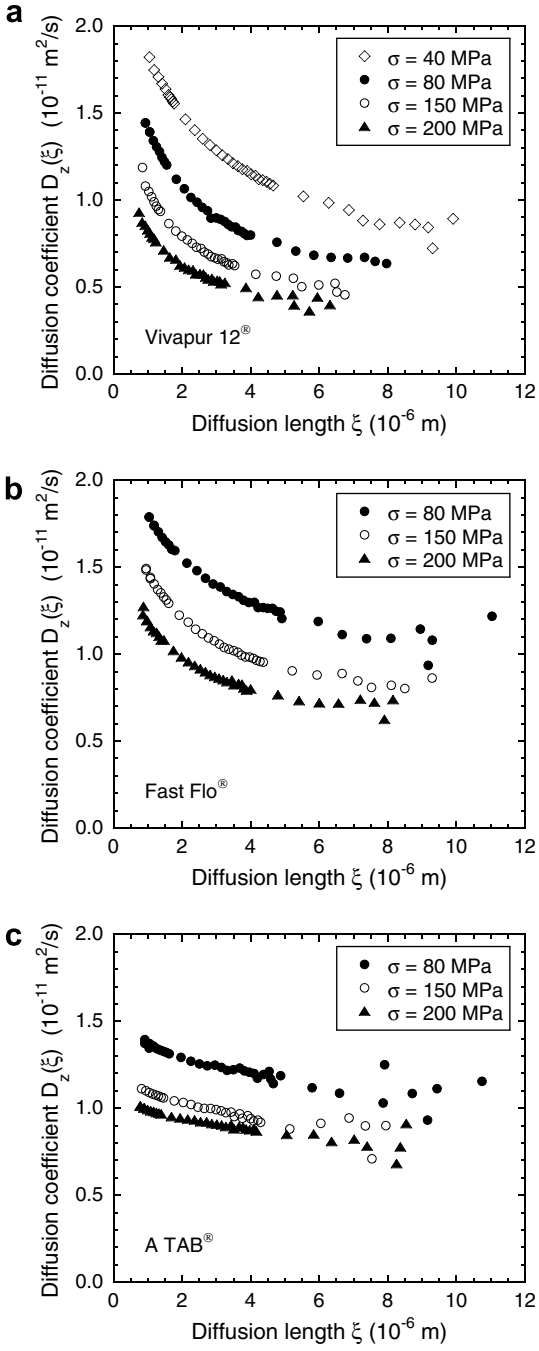


Fig. 9. Evolution of proton self-diffusion coefficient $D_z(\xi)$ with the diffusion length ($\xi$) in the direction ($Oz$) parallel to the compression axis for tablets obtained under different compaction pressure ($\sigma$, MPa); (a) microcrystalline cellulose, (b) lactose and (c) anhydrous calcium phosphate.

by the fluid to travel among the pores between the two parallel planes, perpendicular to the mean flow, is $\theta$ times greater than the straight Enclidean length $L$ separating these planes, $\theta = L^*/L$ is a dimensionless number. The tortuosity is equal to one when the porous structure is made of parallel infinite linear tubes, but it becomes higher than one when the porous structure becomes different of linear porosity (see Fig. 10). For example, in a porous material composed by monodisperse beads, the tortuosity $\theta$ is equal to $\pi/2$. From the PGSTE-NMR measurements, the diffusion coefficient measured at long observation times can be used to estimate another parameter, the tortuosity factor defined as $\tau_i = D_0/D_i^{\infty}$ in the direction $\mathbf{e}_i$ [26,27]. In anisotropic materials, in a given direction $\mathbf{e}_i$, the tortuosity $\theta$ and the tortuosity factor $\tau$ of the pore space are then related to the self-diffusion coefficients by the following equation:

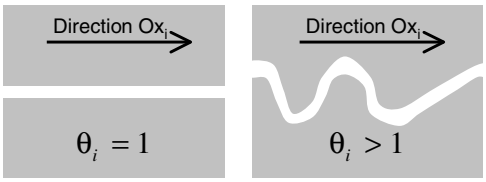


Fig. 10. The tortuosity $\theta$ characterizes the trajectory of a fluid (or the molecules for a gaseous phase) in a porous material. More $\theta$ is large, more the trajectory deviates from the straight line to cross the sample.

$$\theta_i^2 = \tau_i = D_0/D_i^\infty \tag{3}$$

where $D_0$ is the self-diffusion of the fluid in the bulk situation (*i.e.* when it is not confined to the pores space, $D_0 = 2.73 \times 10^{-11}\ \mathrm{m^2\ s^{-1}}$) and $D_i^\infty$ with $i \in \{x,z\}$ corresponds to the macroscopic self-diffusion value as previously defined. This tortuosity factor depends on the connectivity of the pore space and also on the pore size distribution. Furthermore, it may also include some chemi- or physi-sorption effects.

The evolution of the tortuosity factor of the pore space in the two studied directions (*i.e.* $\tau_x$ and $\tau_z$) with the change of the compaction pressure is shown in Fig. 11. For the microcrystalline cellulose tablets, $\tau_z$ is higher than $\tau_x$. More, the difference between the two directions increases with the compaction pressure. $\tau_z$ continuously increases, whereas $\tau_x$ reaches a constant value above a compaction pressure of 100 MPa. At the maximal compaction pressure (*i.e.* $\sigma = 200$ MPa), $\tau_z$ is almost twice $\tau_x$. For lactose and anhydrous calcium phosphate tablets, the tortuosity factor is almost the same in the ($Ox$) and ($Oz$) directions. In the case of lactose, the tortuosity factor increases with the compaction pressure. For anhydrous calcium phosphate, $\tau$ reaches a constant value for a compaction pressure above 150 MPa. Then, concerning the tortuosity factor, an anisotropy of the pore space is observed in the case of microcrystalline cellulose tablets. For the two other excipients, the tortuosity factor shows a homogeneity of the pore space since no variations are observed.

### 3.4. Quantification of the anisotropy of the pore space

The structural anisotropy of the pore space can also be characterized by a simple evaluation of the diffusion anisotropy factor $\lambda$ defined as the ratio:

$$\lambda = D_{\max}^\infty / D_{\min}^\infty \tag{4}$$

where $D_{\max}^\infty$ and $D_{\min}^\infty$ are, respectively, the maximal and minimal value of the macroscopic self-diffusion measured along the two principal directions ($Ox$) and ($Oz$).

When the pore space is isotropic, $D_{\max}^\infty = D_{\min}^\infty = D^\infty$ and $\lambda = 1$. This diffusion anisotropy factor $\lambda$ is expected to increase with the anisotropy of the pore space. The variations of $\lambda$ with the compaction pressure are shown in Fig. 12. For the tablets of microcrystalline cellulose, $\lambda$ is greatly higher than 1 for all compaction pressures. This shows an anisotropy of the porous structure. More, for a compaction pressure higher than 80 MPa (*i.e.* higher than the mean yield pressure), $\lambda$ increases with the compaction pressure. The structure of the pore space is probably different due to a different behaviour of the microcrystalline cellulose particles. For a pressure higher than $P_y$, the microcrystalline cellulose particles deform plastically. This could explain that the anisotropy is more important for the highest compaction pressures. For lactose and anhydrous calcium phosphate tablets, $\lambda$ is almost equal to 1. Then, it can be concluded that the pore structure is isotropic.

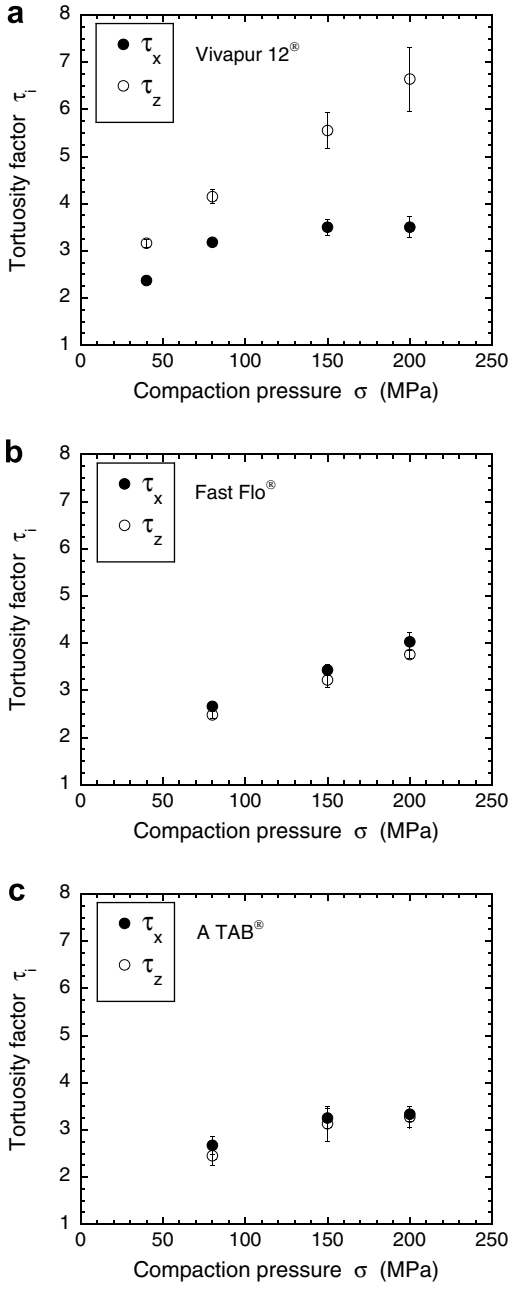


Fig. 11. Tortuosity factor of the pore space *versus* the compaction pressure ($\sigma$, MPa) in the direction perpendicular to the compression axis ($\tau_x$: •) and parallel to the compression axis ($\tau_z$: ○); (a) microcrystalline cellulose, (b) lactose and (c) anhydrous calcium phosphate.

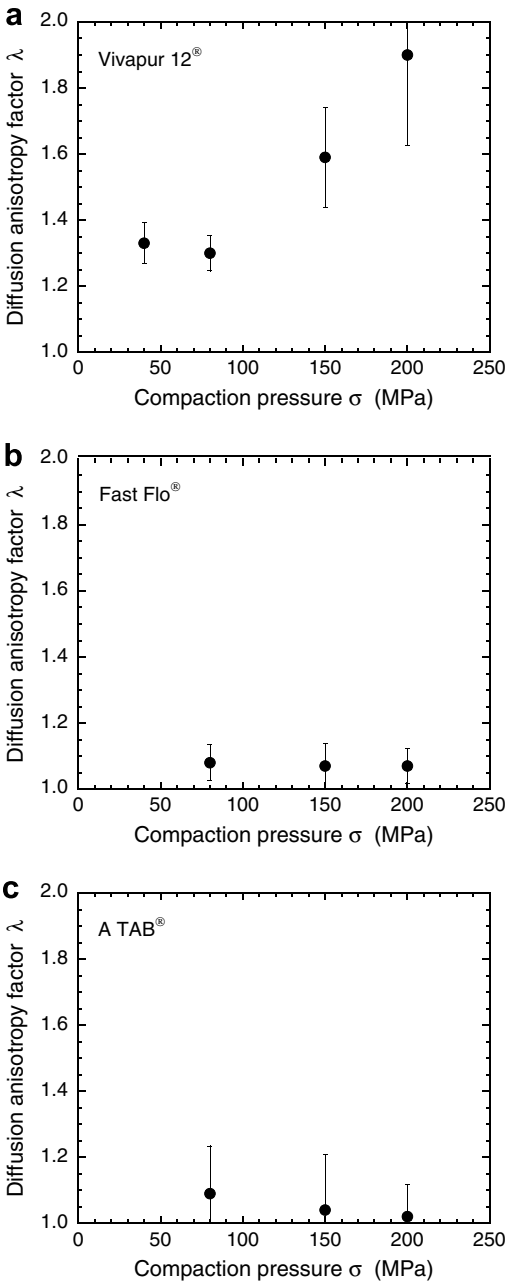


Fig. 12. Evolution of the diffusion anisotropy factor ($\lambda$) with the compaction pressure ($\sigma$, MPa); (a) microcrystalline cellulose, (b) lactose and (c) anhydrous calcium phosphate.

## 4. Conclusion

The compaction step can lead to a heterogeneity of densities and porosity inside the tablets. PGSTE-NMR technique could be an alternative to characterize the pore space of pharmaceutical tablets. More, one of its advantages is that it is a non-destructive technique. Our results show that the diffusion in the pore space depends on the compaction behaviour of the materials used to form tablets. With a plastic material like microcrystalline cellulose in this work, anisotropy of the diffusion parameters is observed. Then, it could be concluded that the pore space of such tablets is anisotropic. On the contrary, for the two other excipients of this work (*i.e.* lactose, an intermediate material and anhydrous calcium phosphate, a brittle excipient), the results of diffusion are that the pore space seems more isotropic in this case. This anisotropy of the pore space is expected to have an effect on some tablet's properties. An exponential relationship between the porosity and some mechanical properties is commonly used [28]. Then, if the pore space is anisotropic, this means that the tablets could exhibit different mechanical property values when measured in different directions [29]. Tablet disintegration, hydration of matrix systems and drug release could also be dependent on an anisotropy of the porous structure [30].

## Acknowledgement

The Bruker DSX100 NMR spectrometer and the Bruker Micro5 microimaging probehead used in this study were purchased, thanks to grants from the CNRS and the Région Centre (France).

## References

[1] D. Train, An investigation into the compaction of powders, J. Pharm. Pharmacol. 8 (1956) 745–761.
[2] G. Nebgen, D. Gross, V. Lehmann, F. Müller, $^{1}$H NMR microscopy of tablets, J. Pharm. Sci. 84 (1995) 283–291.
[3] I.C. Sinka, S.F. Burch, J.H. Tweed, J.C. Cunningham, Measurement of density variations in tablets using X-ray computed tomography, Int. J. Pharm. 271 (2004) 215–224.
[4] V. Busignies, B. Leclerc, P. Porion, P. Evesque, G. Couarraze, P. Tchoreloff, Quantitative measurements of localized density variations in cylindrical tablets using X-ray microtomography, Eur. J. Pharm. Biopharm. 64 (2006) 38–50.
[5] A. Djemai, I.C. Sinka, NMR imaging of density distributions in tablets, Int. J. Pharm. 319 (2006) 55–62.
[6] S.P. Rigby, R.S. Fletcher, J.H. Raistrick, S.N. Riley, Characterisation of porous solids using a synergistic combination of nitrogen sorption, mercury porosimetry, electron microscopy and micro-focus X-ray imaging techniques, Phys. Chem. Chem. Phys. 4 (2002) 3467–3481.
[7] S. Brunauer, P.H. Emmett, E. Teller, Adsorption of gases in multimolecular layers, J. Am. Chem. Soc. 60 (1938) 309–319.
[8] E.P. Barrett, L.G. Joyner, P.P. Halenda, The determination of pore volume and area distributions in porous substances. I. Computations from nitrogen isotherms, J. Am. Chem. Soc. 73 (1951) 373–380.
[9] P.T. Callaghan, Principles of Nuclear Magnetic Resonance Microscopy, Clarendon Press, Oxford, 1991.
[10] T. Watson, P. Chang, Characterizing porous media with NMR methods, Prog. Nucl. Magn. Reson. Spectrosc. 31 (1997) 343–386.
[11] R. Ek, T. Gren, U. Henriksson, H. Nyqvist, C. Nyström, L. Ödberg, Prediction of drug release by characterization of the tortuosity in porous cellulose beads using a spin echo NMR technique, Int. J. Pharm. 124 (1995) 9–18.
[12] P. Porion, M. Al-Mukhtar, A.M. Faugère, R.J.M. Pellenq, S. Meyer, A. Delville, Water self-diffusion within nematic dispersion of nanocomposites: a multiscale analysis of $^{1}$H pulsed gradient spin-echo NMR measurements, J. Phys. Chem. B 107 (2003) 4012–4023.
[13] P. Porion, M. Al-Mukhtar, A.M. Faugère, A. Delville, $^{23}$Na nuclear magnetic resonance and $^{1}$H pulsed gradient spin-echo detection of the critical concentration corresponding to the isotope/nematic transition within aqueous dispersions of charged anisotropic nanoparticles, J. Phys. Chem. B 108 (2004) 10825–10831.

[14] E. Doelker, Comparative compaction properties of various microcrystalline cellulose types and generic products, Drug. Dev. Ind. Pharm. 19 (1993) 2399–2471.
[15] C. Doldan, C. Souto, A. Concheiro, R. Martinez-Pacheco, J.L. Gomez-Amoza, Dicalcium phosphate dihydrate and anhydrous dicalcium phosphate for direct compression: a comparative study, Int. J. Pharm. 124 (1995) 69–74.
[16] T. Sebhatu, C. Ahlneck, G. Alderborn, The effect of moisture content on the compression and bond formation properties of amorphous lactose particles, Int. J. Pharm. 146 (1997) 101–114.
[17] V. Busignies, B. Leclerc, P. Porion, P. Evesque, G. Couarraze, P. Tchoreloff, Compaction behaviour and new predictive approach to the compressibility of binary mixtures of pharmaceutical excipients, Eur. J. Pharm. Biopharm. 64 (2006) 66–74.
[18] V. Busignies, P. Tchoreloff, B. Leclerc, M. Besnard, G. Couarraze, Compaction of crystallographic forms of pharmaceutical granular lactoses. I. Compressibility, Eur. J. Pharm. Biopharm. 58 (2004) 569–576.
[19] W. Heckel, An analysis of powder compaction phenomena, Trans. Metal. Soc. A.I.M.E. 221 (1961) 671–675.
[20] W. Heckel, Density-pressure relationship in powder compaction, Trans. Metal. Soc. A.I.M.E. 221 (1961) 1001–1008.
[21] E.O. Stejskal, J.E. Tanner, Spin diffusion measurements: spin echoes in the presence of a time-dependent field gradient, J. Chem. Phys. 42 (1965) 288–292.
[22] J.E. Tanner, Use of the stimulated echo in NMR diffusion studies, J. Chem. Phys. 52 (1970) 2523–2526.
[23] P.T. Callaghan, A. Coy, T.P.J. Halpin, D. MacGowan, K.J. Packer, F.O. Zelaya, Diffusion in porous systems and the influence of pore morphology in pulsed gradient spin-echo nuclear magnetic resonance studies, J. Chem. Phys. 97 (1992) 651–662.
[24] V. Busignies, B. Leclerc, P. Porion, P. Evesque, G. Couarraze, P. Tchoreloff, Application of percolation model to the tensile strength and the reduced modulus of elasticity of three compacted pharmaceutical excipients, Eur. J. Pharm. Biopharm. 67 (2007) 507–514.
[25] P.C. Carman, Fluid flow through granular beds, Trans. Inst. Chem. Eng. 15 (1937) 150–166.
[26] L.L. Latour, R.L. Kleinberg, P.P. Mitra, C.H. Sotak, Pore-size distribution and tortuosity in heterogeneous porous media, J. Magn. Reson. A 112 (1995) 83–91.
[27] A.S. Kim, H. Chen, Diffusive tortuosity factor of solid and soft cake layers: a random walk simulation approach, J. Membr. Sci. 279 (2006) 129–139.
[28] W.H. Duckworth, Discussion of Ryshkewitch paper by Winston Duckworth, J. Am. Ceram. Soc. 36 (1953) 68.
[29] M.P. Mullarney, B.C. Hancock, Mechanical property anisotropy of pharmaceutical excipient compacts, Int. J. Pharm. 314 (2006) 9–14.
[30] J.C. Richardson, R.W. Bowtell, K. Mäder, C.D. Melia, Pharmaceutical applications of magnetic resonance imaging (MRI), Adv. Drug Deliv. Rev. 57 (2005) 1191–1209.